

Faculty Scholarship

7-13-2022

Antithrombin-III Mitigates Thrombin-Mediated Endothelial Cell Contraction and Sickle Red Blood Cell Adhesion in Microscale Flow

William J. Wulftange

Case Western Reserve University, william.wulftange@case.edu

Erdem Kucukal

Case Western Reserve University

Yuncheng Man

Case Western Reserve University

Ran An

Case Western Reserve University, ran.an4@case.edu

Karamoja Monchamp

Case Western Reserve University

~~See next page for additional authors~~

Follow this and additional works at: <https://commons.case.edu/facultyworks>



Part of the [Hematology Commons](#)

Recommended Citation

Wulftange, William J.; Kucukal, Erdem; Man, Yuncheng; An, Ran; Monchamp, Karamoja; Sevrain, Charlotte D.; Dashora, Himanshu R.; Bode, Allison; Little, Jane A.; and Gurkan, Umut A., "Antithrombin-III Mitigates Thrombin-Mediated Endothelial Cell Contraction and Sickle Red Blood Cell Adhesion in Microscale Flow" (2022). *Faculty Scholarship*. 99.

<https://commons.case.edu/facultyworks/99>







This Article is brought to you for free and open access by Scholarly Commons @ Case Western Reserve University. It has been accepted for inclusion in Faculty Scholarship by an authorized administrator of Scholarly Commons @ Case Western Reserve University. For more information, please contact digitalcommons@case.edu.

Authors

William J. Wulftange, Erdem Kucukal, Yuncheng Man, Ran An, Karamoja Monchamp, Charlotte D. Sevrain, Himanshu R. Dashora, Allison Bode, Jane A. Little, and Umut A. Gurkan

ORIGINAL PAPER

Antithrombin-III mitigates thrombin-mediated endothelial cell contraction and sickle red blood cell adhesion in microscale flow

William J. Wulftange¹  | Erdem Kucukal¹ | Yuncheng Man¹  | Ran An¹  |
 Karamoja Monchamp¹ | Charlotte D. Sevrain¹ | Himanshu R. Dashora¹ |
 Amma T. Owusu-Ansah² | Allison Bode¹ | Anton Ilich³  | Jane A. Little³ |
 Nigel S. Key³  | Umut A. Gurkan^{1,4,5} 

¹Department of Mechanical and Aerospace Engineering, Case Western Reserve University, Cleveland, Ohio, USA

²Department of Pediatrics, Division of Hematology Oncology, University Hospitals Rainbow Babies and Children's Hospital, Cleveland, Ohio, USA

³Division of Hematology and UNC Blood Research Center, Department of Medicine, University of North Carolina, Chapel Hill, North Carolina, USA

⁴Department of Biomedical Engineering, Case Western Reserve University, Cleveland, Ohio, USA

⁵Case Comprehensive Cancer Center, Case Western Reserve University, Cleveland, Ohio, USA

Correspondence

Umut A. Gurkan, Department of Mechanical and Aerospace Engineering, Department of Biomedical Engineering, Case Comprehensive Cancer Center, Case Western Reserve University, Office: Glennan 616B, 10900 Euclid Ave., Cleveland, OH 44106, USA. Email: umut@case.edu

Funding information

Division of Civil, Mechanical and Manufacturing Innovation, Grant/Award Number: CAREER Award 1552782; National Center for Advancing Translational Sciences, Grant/Award Number: UL1TR002548; National Heart, Lung, and Blood Institute, Grant/Award Number: OT2HL152643, R01HL133574, T32HL134622 and U01HL117659; National Institute of General Medical Sciences, Grant/Award Number: T32GM007250 and TL1TR000441; Grifols; Case-Coulter Translational Research Partnership Program; NIH Roadmap for Medical Research

Summary

Individuals with sickle cell disease (SCD) have persistently elevated thrombin generation that results in a state of systemic hypercoagulability. Antithrombin-III (ATIII), an endogenous serine protease inhibitor, inhibits several enzymes in the coagulation cascade, including thrombin. Here, we utilize a biomimetic microfluidic device to model the morphology and adhesive properties of endothelial cells (ECs) activated by thrombin and examine the efficacy of ATIII in mitigating the adhesion of SCD patient-derived red blood cells (RBCs) and EC retraction. Microfluidic devices were fabricated, seeded with ECs, and incubated under physiological shear stress. Cells were then activated with thrombin with or without an ATIII pretreatment. Blood samples from subjects with normal haemoglobin (HbAA) and subjects with homozygous SCD (HbSS) were used to examine RBC adhesion to ECs. Endothelial cell surface adhesion molecule expression and confluency in response to thrombin and ATIII treatments were also evaluated. We found that ATIII pretreatment of ECs reduced HbSS RBC adhesion to thrombin-activated endothelium. Furthermore, ATIII mitigated cellular contraction and reduced surface expression of von Willebrand factor and vascular cell adhesion molecule-1 (VCAM-1) mediated by thrombin. Our findings suggest that, by attenuating thrombin-mediated EC damage and RBC adhesion to endothelium, ATIII may alleviate the thromboinflammatory manifestations of SCD.

KEY WORDS

antithrombin, coagulation, microfluidics, sickle cell disease, thrombin, vascular endothelium

This is an open access article under the terms of the [Creative Commons Attribution-NonCommercial](https://creativecommons.org/licenses/by-nc/4.0/) License, which permits use, distribution and reproduction in any medium, provided the original work is properly cited and is not used for commercial purposes.

© 2022 The Authors. *British Journal of Haematology* published by British Society for Haematology and John Wiley & Sons Ltd.

INTRODUCTION

Chronic activation of coagulation is a characteristic feature of sickle cell disease (SCD).^{1,2} For patients with SCD in both steady state and active painful crises, previous studies have shown chronically elevated levels of endogenous thrombin generation, depleted natural anticoagulants, and abnormal activation of fibrinolysis.³ Abnormally enhanced adhesion of haematopoietic cells with associated vascular inflammation are also typical of SCD.^{4,5}

Recent studies have identified a multitude of potential therapeutic targets in SCD, particularly with respect to the coagulation cascade.⁶⁻¹⁰ One promising target is thrombin, a key enzyme that is generated through the cleavage of factor II (prothrombin) via the prothrombinase complex formed by factors Xa and Va in a membrane-dependent interaction.^{11,12} Thrombin generation has shown to be elevated in patients with SCD and contributes to microvascular stasis in murine models of SCD.¹³ Additionally, thrombin-activated ECs increase HbSS RBC adhesion through EC surface proteins and subendothelial matrix interactions.^{14,15} Despite the major role thrombin plays in SCD and several ongoing clinical trials, there are no FDA-approved therapeutic options that target this crucial step in the coagulation cascade.^{13,16,17} The serpin ATIII inhibits several coagulation enzymes, including thrombin, and its activity is greatly enhanced when the enzyme binds to pharmacologic heparin or heparan sulphate molecules located on the surface of endothelial cells (ECs).¹⁸ Since thrombin has shown to play a critical role in SCD, in this study we sought to investigate whether or not ATIII could mitigate thrombin-mediated HbSS adhesion.¹³⁻¹⁵

In this work, we utilized a biomimetic endothelium-on-a-chip microfluidic assay to assess the effect of ATIII on the morphology and function of human ECs activated by human alpha thrombin. The endothelium-on-a-chip microfluidic assay functions as a platform on which human ECs are cultured under physiological shear stress. This system permits the perfusion of patient blood samples to assess *in vitro* characteristics in comparison to clinical pathologies and phenotypes.¹⁹⁻²² Here, we focused on modelling morphology and adhesive properties of ECs activated by human alpha thrombin. Our findings show that thrombin activation leads to significant changes in EC morphology as well as enhanced adhesion of RBCs from subjects homozygous for HbS. Notably, pretreatment of ECs with

ATIII prior to thrombin activation prevented both EC contraction and RBC adhesion. Summarily, these results demonstrate the efficacy of ATIII in preventing EC damage and consequent adhesive interplay between ECs and RBCs in SCD.

METHODS

Subjects and blood sample collection

Whole-blood samples were obtained from de-identified adult subjects with or without HbSS SCD at University Hospitals CWRU (Cleveland, OH, USA), under an Institutional Review Board-approved protocol. Samples were collected in ethylenediaminetetra-acetic acid (EDTA)-containing tubes and used within two days of collection. Subjects with HIV or hepatitis C were ineligible for this study. Clinical phenotypes of individual patients are shown in Table S1.

Endothelium-on-a-chip fabrication and microchannel endothelialization

Microfluidic devices were fabricated according to our previously published methods.¹⁹ Microchannel geometry was formed via a laser micro-machined double-sided adhesive film (DSA film, 3M, Saint Paul, MN, USA) placed between a microscope glass slide and a polymethyl methacrylate block (PMMA, McMaster-Carr, Elmhurst, IL, USA) with inlet and outlet holes (Figure 1A). Assembled microchannels were rinsed with phosphate-buffered saline (PBS, Gibco, Life Technologies, Thermo Fisher Scientific, Waltham, MA, USA), 100% ethanol, and functionalized by incubation with *N*- γ -maleimidobutryl-oxysuccinimide ester (GMBS, Thermo Fisher, Waltham, MA, USA) for 20 min at room temperature. Following a PBS wash step, a 0.2 mg/ml fibronectin (Sigma-Aldrich, St. Louis, MO, USA) solution was perfused into each microchannel and incubated at 37°C for 1 h. Thereafter, human umbilical vein endothelial cells (HUVECs, Lonza Inc., Morristown, NJ, USA) were seeded into the microchannels at a density of 8×10^6 cells/ml and incubated at 37°C and 5% CO₂ for 10 mins, after which the seeding process was repeated and the microchannels were incubated at 37°C and 5% CO₂ for another hour. Each microfluidic chip was then connected in tandem to a

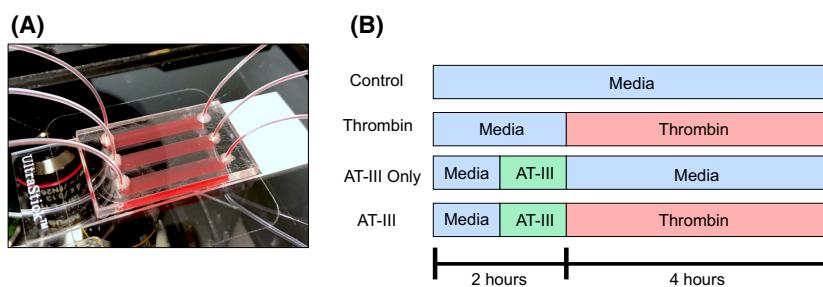


FIGURE 1 Overview of microfluidic device and experimental design. (A) Endothelium-on-a-chip is shown during a sickle cell blood adhesion assay. (B) Illustration of experimental design for various microchannel conditions. Each bar represents static incubation solution following culturing each device under flow. [Colour figure can be viewed at wileyonlinelibrary.com]

flow system that perfused fresh culture medium [EGM, 2% fetal bovine serum (FBS), Lonza Inc., Morristown, NJ, USA] at a rate of 150 $\mu\text{l}/\text{min}$ over the cells. Following the perfusion culture for 24 h, the culture medium was replaced with serum-free ITS+1 (insulin–transferrin–selenium–linoleic acid–bovine serum albumin, Thermo Fisher Scientific, Waltham, MA, USA) containing EGM culture medium overnight, prior to the day of experimentation.

Thrombin activation and ATIII treatment of endothelial cells

Microfluidic chips were disconnected from flow followed by treatment of cells with appropriate media. Control cells were perfused with ITS+1 medium alone. Thrombin microchannels were perfused with 5 u/ml human alpha thrombin (Haemtech, Essex, VT, USA) in ITS+1 medium. For ATIII pretreatment, 7 u/ml ATIII in ITS+1 medium was perfused into microchannels and incubated at 37°C and 5% CO_2 for 1 h and washed prior to thrombin addition. The experimental design conditions are illustrated in [Figure 1B](#). The microfluidic devices were then incubated at 37°C and 5% CO_2 for the duration of the experiment, with media being replaced every 2 h if necessary. ATIII was donated by Grifols USA (Los Angeles, CA, USA).

Immunofluorescence analysis of endothelial cells

Immediately following incubation, each microchannel was perfused with 3.7% formalin and incubated for 10 mins at room temperature. The microchannels were then washed thrice with PBS to remove the formalin solution. Next, bovine serum albumin (BSA) was perfused into each microchannel followed by a 4°C incubation overnight. BSA was then removed using serial washes of PBS. Fluorescently conjugated antibodies against human intercellular cell adhesion molecule-1 (ICAM-1) (0.25 $\mu\text{g}/\text{ml}$), P-selectin (0.125 $\mu\text{g}/\text{ml}$), and von Willebrand factor (vWF, 20 $\mu\text{g}/\text{ml}$) were diluted in 1% BSA solution and injected into the microchannels. Following a 1-h incubation at room temperature, the microchannels were rinsed thrice with PBS. For VCAM-1 (1 $\mu\text{g}/\text{ml}$) and VE-cadherin (0.2825 $\mu\text{g}/\text{ml}$) staining, primary antibodies were diluted in 1% BSA solution and injected into the microchannels. Channels were incubated at 4°C overnight and then rinsed thrice with PBS. Fluorescently conjugated secondary antibodies were then diluted in 1% BSA solution and Hoechst 33342 (1 $\mu\text{g}/\text{ml}$), injected into the microchannels, and incubated for 2 h at room temperature. Following incubation, microchannels were rinsed thrice with PBS. Phase contrast and fluorescence images of the mounted cells were acquired via an inverted microscope at 20 \times (Olympus, IX83).

Red blood cell adhesion assay

Whole-blood samples were collected from both HbAA and HbSS SCD patients and kept at 4°C until ready for use. The

samples were used within the first 24 h after venipuncture unless stated otherwise. For the adhesion experiments, red blood cells (RBCs) were isolated from whole blood by centrifuging at 500 g for 5 min followed by aspiration of the plasma and buffy coat. Isolated RBCs were then washed twice with PBS at 500 g for 5 min and resuspended in basal cell culture medium supplemented with 15 mM HEPES (Vasculife, Lifeline Cell Technology, Frederick, MD, USA) at a haematocrit of 20% for HbSS samples and 40% for HbAA samples. Microfluidic channels were rinsed with HEPES-buffered basal media prior to the adhesion experiments to remove experimental solutions. Inlet lines filled with HEPES-buffered basal medium were then connected to inlets on microfluidic devices and sealed with epoxy. The samples were then drawn into 1-ml syringes that were attached to the inlet lines of the microfluidic devices. Next, the sample-containing syringes were placed on a multiple syringe pump, through which the samples were perfused over the ECs at a flow rate of 1.85 $\mu\text{l}/\text{min}$ (~ 1 dyne/ cm^2) for a total of 15 μl . Thereafter, the microfluidic channels were rinsed with HEPES-buffered medium at a rate of 10 $\mu\text{l}/\text{min}$ (~ 1 dyne/ cm^2) to remove unbound RBCs. Finally, a 32- mm^2 field of view was scanned at 10 \times in the middle of the microchannel for subsequent image analysis.

ImageJ analysis of confluency

For confluency measurements, phase-contrast images were analysed using the PHANTAST plugin of ImageJ with default settings.²³ Empty microchannel space was outlined in yellow ([Figure 2](#)). Fluorescence intensity was determined by measuring the colour intensity values of multiple regions from multiple experiments for each condition and adjusting for cellular confluency.

Statistical methods

Data acquired in this study were reported as the mean \pm standard error of the mean. All statistical analyses were performed using GraphPad Prism 8 software (GraphPad Holdings, LLC). Parametric data were analysed using a one-way analysis of variance (ANOVA) followed by Tukey's multiple comparisons test. For parametric comparisons between two groups, an unpaired *t*-test was used. Statistical significance was set at 95% confidence interval for all tests ($p < 0.05$). Asterisks are used for significance levels: *, $p \leq 0.05$; **, $p \leq 0.005$; ***, $p \leq 0.0005$; ****, $p \leq 0.0001$.

RESULTS

ATIII mitigates endothelial contraction mediated by thrombin

When incubated with 5 u/ml thrombin for 4 h, HUVECs underwent cellular contraction as summarized in [Figure 2](#). HUVECs incubated with ITS+1 media had an average

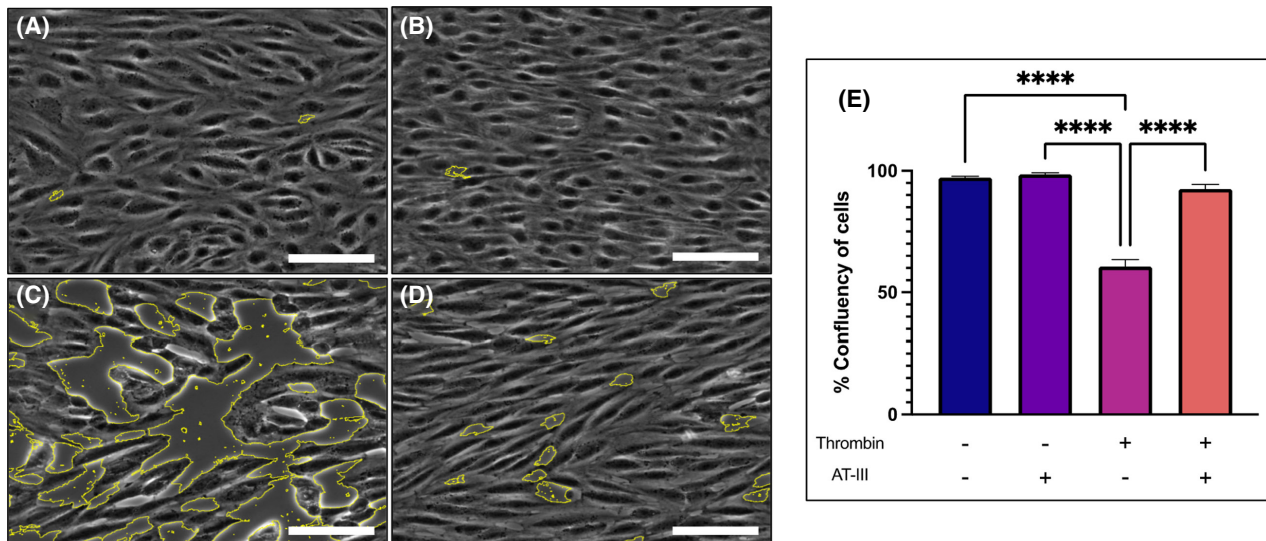


FIGURE 2 Antithrombin-III (AT-III) prevents a thrombin-mediated cellular contraction. Confluency of control channels is near total, but decreases by nearly half when incubated with thrombin 5 u/ml for 4 h. This contracted phenotype is prevented by pretreating with AT-III 7 u/ml for 1 h prior to thrombin treatment. Representative images of (A) the control, (B) AT-III without thrombin, (C) thrombin 5 u/ml, (D) and thrombin with AT-III. Channels are shown with empty channel space outlined in yellow. Scale bars represent 100 μ m. (E) Overall confluency of endothelial cells under control and treated conditions with relevant significance displayed. Asterisks are used for significance levels: *, $p \leq 0.05$; **, $p \leq 0.005$; ***, $p \leq 0.0005$; **** $p \leq 0.0001$. Data were analysed using a one-way analysis of variance (ANOVA) followed by Tukey's multiple comparisons test. [Colour figure can be viewed at [wileyonlinelibrary.com](https://onlinelibrary.wiley.com)]

confluency of $97.2 \pm 0.5\%$ (Figure 2A). When treated with ATIII alone, HUVEC confluency was $98.5 \pm 0.7\%$ (Figure 2B), while thrombin-treated HUVECs displayed an average confluency of only $58.9 \pm 1.8\%$, which was significantly lower than the control (Figure 2C, $n = 9$ for controls, $n = 8$ for ATIII only, and $n = 6$ for thrombin channels, $p < 0.0001$). This contraction could be prevented by incubating the microchannels with 7 u/ml ATIII for 1 h prior to washing and incubation with thrombin. Specifically, pretreatment of HUVECs with ATIII resulted in a cell confluency of $92.5 \pm 1.8\%$, which was significantly increased compared to no ATIII pretreatment (Figure 2D, $n = 7$ for ATIII channels, $p < 0.0001$).

We also evaluated the effect of a shorter duration of thrombin exposure. A 15-min incubation with thrombin resulted in an average confluency of $94.4 \pm 3.1\%$, with ATIII pretreatment producing an average confluency of $96.3\% \pm 0.9$ ($n = 3$ for thrombin and $n = 3$ for ATIII channels, $p = 0.59$). Contraction of HUVECs under these conditions is illustrated in Figure S1A,B. The overall results of confluency experiments are shown in Figure S1C. We also conducted cellular contraction experiments with a second cell line, human pulmonary microvascular endothelial cells (HPMVECs), and observed the same trends as shown in Figure S2.

Thrombin does not significantly increase HbAA RBC adhesion

To determine whether thrombin activation with or without ATIII pretreatment affects HbAA RBC interactions with ECs, we perfused HbAA RBC suspensions over the treated

endothelial monolayers. Adhesion of HbAA RBCs was expectedly low since these cells are generally non-adhesive to endothelium.²⁴ Control channels had an average of 2.5 ± 0.83 RBCs (Figure 3A, $n = 4$) per analysed region (32 mm^2). AT-III pretreatment alone did not significantly change the adhesion levels, with an average of 3.6 ± 0.7 RBCs per analysed region (Figure 3B, $n = 4$). Thrombin-activated endothelium had a slightly higher average of 15.7 ± 5.4 RBCs per analysed region, but this was only significantly different from AT-III only (Figure 3C, $n = 8$ for AT-III only channels, $p = 0.0473$). Finally, AT-III pretreatment followed by thrombin exposure had an average of 4.0 ± 1.1 adherent RBCs per analysed region (Figure 3D, $n = 4$ for AT-III channels). Aside from the sole significant difference between ATIII alone and thrombin only channels, no significant differences were noted, illustrating that HbAA RBC adhesion to both quiescent and activated ECs was limited. A complete comparison of these data is shown in Figure 3E.

ATIII reduces sickle red blood cell adhesion on thrombin-activated endothelium

Since RBC adhesion plays a crucial role in SCD pathophysiology, we next evaluated adhesion of RBCs to HUVECs, treated with thrombin and/or ATIII, using blood samples from individuals with homozygous SCD. We found that HbSS RBCs adhered to quiescent ECs at an average of 16.0 ± 9.8 RBCs per region (Figure 3F, $n = 4$ for control channels) and to ECs treated with ATIII only at an average of 14.3 ± 3.6 RBCs per region (Figure 3G, $n = 10$ for ATIII only channels). Both of these conditions had significantly

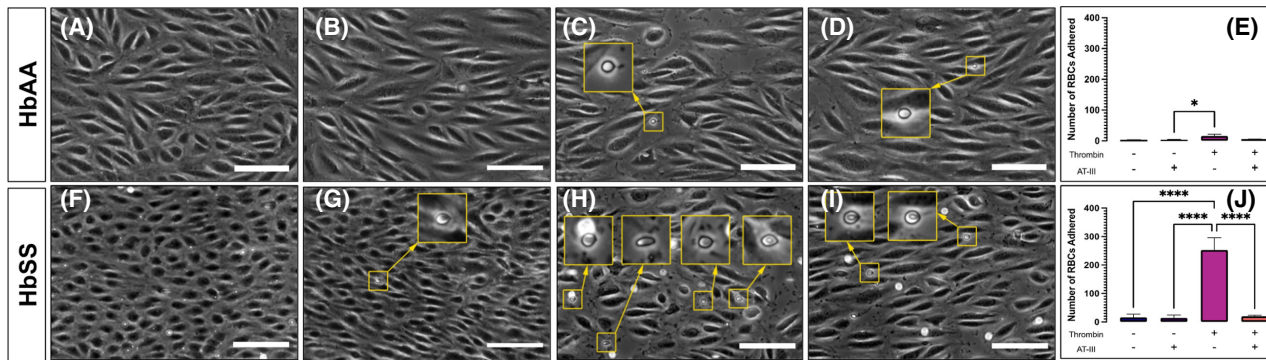


FIGURE 3 HbSS red blood cell (RBC) adhesion to endothelium is increased through thrombin activation and can be prevented with antithrombin III (AT-III) pretreatment. Representative images of endothelium after perfusion of HbAA RBCs are shown for the following conditions: (A) control; (B) AT-III without thrombin; (C) thrombin 5 u/ml; and (D) thrombin with AT-III. (E) Number of HbAA RBCs adhered to endothelial cells following control and treated conditions. For endothelium with adherent HbSS RBCs, the following representative images are shown for: (F) control; (G) AT-III without thrombin; (H) thrombin 5 u/ml; and (I) thrombin with ATIII. (J) Number of HbSS RBCs adhered to endothelial cells following control and treated incubation conditions. Adherent RBCs are enlarged for clarity and outlined in yellow. Adherent cells not outlined are leukocytes. Scale bars represent 100 μ m. Asterisks are used for significance levels: *, $p \leq 0.05$; **, $p \leq 0.005$; ***, $p \leq 0.0005$; ****, $p \leq 0.0001$. Data were analysed using a one-way analysis of variance (ANOVA) followed by Tukey's multiple comparisons test. [Colour figure can be viewed at [wileyonlinelibrary.com](https://onlinelibrary.wiley.com)]

lower adhesion levels compared to thrombin-activated ECs (Figure 3H, $n = 6$ for thrombin-treated channels), which had an average of 252.5 ± 39.6 RBCs per analysed region ($p < 0.0001$ for both comparisons). While thrombin greatly increased levels of HbSS RBC adhesion, ATIII pretreatment significantly lowered thrombin-mediated adhesion to an average of 19.8 ± 3.6 cells (Figure 3I, $n = 9$ for ATIII channels, $p < 0.0001$). These findings and comparisons are summarized in Figure 3J.

ATIII protects endothelium by binding to heparan sulphate

To further investigate the mechanism through which ATIII protects HUVECs from the effects of thrombin, we injected heparinase I (0.5 μ M) into the microchannels and incubated for 1 h prior to ATIII addition in order to degrade heparan sulphate molecules on the HUVEC surface (Figure 4A). Heparinase I prevented ATIII from protecting against thrombin-mediated cellular contraction as shown in Figure 4B,C. These data suggest that ATIII binds to heparan sulphate on the endothelial surface.²⁵

ATIII reduces thrombin-mediated adhesion molecule surface expression

It has been shown that HbSS RBCs adhere to activated ECs through various receptors and ligands such as ICAM-1 and P-selectin.^{13,19,21,22,24,26,27,28} We chose to investigate how thrombin with or without ATIII modulate the surface expression of ICAM-1, P-selectin, and von Willebrand factor (vWF), which may mediate RBC adhesion to the HUVEC surface. We found that thrombin significantly increased surface expression of ICAM-1 following a 4-h treatment compared to quiescent ECs (Figure 5A, $n = 9$ for both

conditions, in arbitrary units (AU), fluorescence intensity (FI) = control: 5.2 ± 0.1 AU vs thrombin: 6.0 ± 0.2 AU, $p = 0.0002$). Surface ICAM-1 expression was attenuated by a 1-h ATIII pre-incubation (Figure 5A, $n = 9$, FI = ATIII: 5.2 ± 0.1 AU vs thrombin: 6.0 ± 0.2 AU, $p = 0.0002$). We also observed that surface P-selectin expression significantly increased in response to thrombin alone but this was not reduced by ATIII pretreatment compared to controls (Figure 5B, $n = 8$ for control, $n = 9$ for thrombin, FI = control: 12.8 ± 1.1 AU vs thrombin: 13.1 ± 0.3 AU, $p = 0.04$. $n = 9$ for thrombin and ATIII, FI = thrombin: 13.1 ± 0.3 AU vs AT-II: 15.0 ± 0.4 AU, $p = 0.003$). Lastly, vWF expression was significantly increased with thrombin exposure, but this increased expression was decreased with ATIII pretreatment (Figure 5C, $n = 8$ for control, $n = 8$ for thrombin, FI = control: 8.6 ± 0.3 AU vs thrombin: 10.0 ± 0.3 AU, $p < 0.0001$; $n = 8$ for thrombin, $n = 9$ for AT-III, FI = thrombin: 10.0 ± 0.3 AU vs AT-II: 9.3 ± 0.1 AU, $p = 0.02$). Representative images of surface expression can be seen in Figure 5D. Fluorescence data for 15-min thrombin experiments are shown in Supplemental Figure S3.

HbSS RBCs have been widely reported to adhere to VCAM-1 molecules on activated endothelial surfaces.²⁸⁻³⁰ Therefore, we investigated the surface VCAM-1 expression as well as the tight junction protein VE-cadherin to further characterize thrombin-activated endothelium. Thrombin-activated endothelial cells expressed significantly more VCAM-1 compared to controls and this expression remained high despite ATIII pretreatment (Figure 6A, $n = 11$ for control, $n = 14$ for thrombin, $n = 13$ for ATIII, FI = Control: 8.7 ± 0.1 AU vs thrombin: 10.9 ± 0.1 AU or vs ATIII: 10.7 ± 0.1 AU, $p < 0.0001$ for both comparisons). We then fluorescently tagged VE-cadherin and observed that thrombin-activated ECs had increased FI ($n = 14$, 41.1 ± 0.4 AU) compared to both control ($n = 11$, 22.7 ± 0.8 AU) and ATIII ($n = 13$, 30.6 ± 0.9 AU) channels ($p < 0.0001$ for all comparisons).

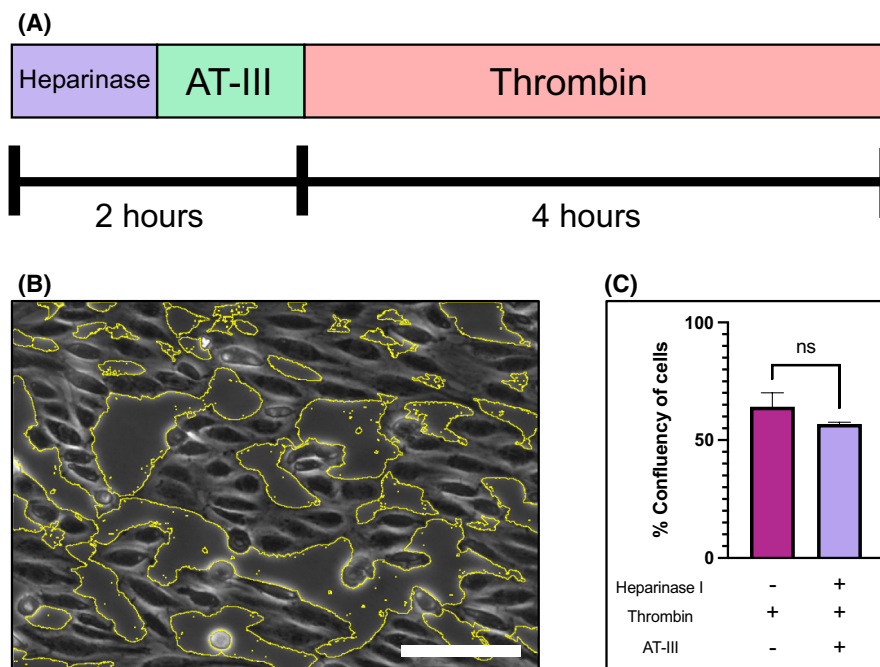


FIGURE 4 Heparinase I inhibits protective effects of antithrombin III (AT-III). (A) Experimental design of heparinase I experiments with bar representing static incubation following culture under flow. (B) Representative image of the cellular contraction seen when heparinase I is used prior to AT-III. Channel is shown with empty channel space outlined in yellow. Scale bar represents 100 μm . (C) Graph of channel confluency showing that heparinase I in combination with AT-III and thrombin is not statistically significant from thrombin alone, suggesting heparinase I counteracts the effects of AT-III. Asterisks are used for significance levels; *, $p \leq 0.05$; **, $p \leq 0.005$; ***, $p \leq 0.0005$; ****, $p \leq 0.0001$. Data were analysed using an unpaired *t*-test. [Colour figure can be viewed at wileyonlinelibrary.com]

DISCUSSION

In SCD, RBCs become aberrantly adhesive and stiff, causing the integrity of the cell membranes to be more fragile and susceptible to lysis.²⁰ Within the microvasculature, adhesion molecules such as VCAM-1, ICAM-1, and selectins facilitate adhesion of blood cells, especially sickled RBCs, to the vascular bed leading to vaso-occlusive events (VOEs).^{21,28,31,32} SCD is also a well-recognized hypercoagulable state characterized by chronic *in vivo* activation of the coagulation cascade and clinically, a higher risk of venous thromboembolic events. Plasma biomarkers in SCD are typically skewed toward a procoagulant state; procoagulants such as thrombin-antithrombin complexes are increased at baseline, while natural anticoagulants such as proteins C and S are decreased.^{33,34} Long-term consequences of hypercoagulability and chronic haemolysis and vaso-occlusion can lead to progressive end-organ damage including, but not limited to, the kidneys, lungs, brain and cardiovascular system.³⁵

In this study, we expanded upon our previous work of using endothelium-on-a-chip to explore assays of HbSS RBC adhesion in a clinically and physiologically relevant manner.^{19,20,22,26} By modelling this disease state *in vitro*, we have studied potential pharmaceutical therapies and prophylactic approaches with patient-specific precision.^{21,22,36} Previously, we demonstrated that the endothelium-on-a-chip device could be used to model pathological haemolytic states by studying haeme-activated endothelium.^{19,36} Currently, we expand upon the translational potential of this microfluidic

platform by testing a biological therapy, ATIII. We have characterized endothelial cell activation and HbSS RBC adhesion before and after the addition of ATIII to activated HUVECs. We hope this work adds to the growing body of literature that demonstrates the utility of microfluidic devices in the drug development pipeline.

Due to the high levels of thrombin generation that have been shown in SCD patients both in steady state and during VOEs, we used human thrombin to activate HUVECs in this work.^{13,16} We treated HUVECs with thrombin at 5 u/ml for several time periods to examine the role of thrombin on endothelial health and cellular adhesion. An obvious phenotype was the cellular contraction that HUVECs displayed. The mechanism of this contraction is detailed in the literature as being caused by myosin light chain-2 phosphorylation.^{31,32} This barrier degradation became visible within 15 mins of incubation but was prominent with increasing incubation time. Increased permeability of vasculature and breakdown of endothelial barriers due to thrombin exposure have been reported in the literature and have also been shown in transgenic mice with SCD.³²⁻³⁴

ATIII is a plasma glycoprotein of the serpin family of protease inhibitors that exerts both anticoagulant effects (as a cofactor for heparin) and anti-inflammatory effects.¹⁸ ATIII's anti-inflammatory effects are mediated through binding of its D-helix to heparan sulphate's proteoglycans on the surface of endothelial cells.³⁵ This interaction leads to the synthesis of prostacyclin, which is a vasodilator, as well as an inhibitor of platelet aggregation, activated macrophages, and

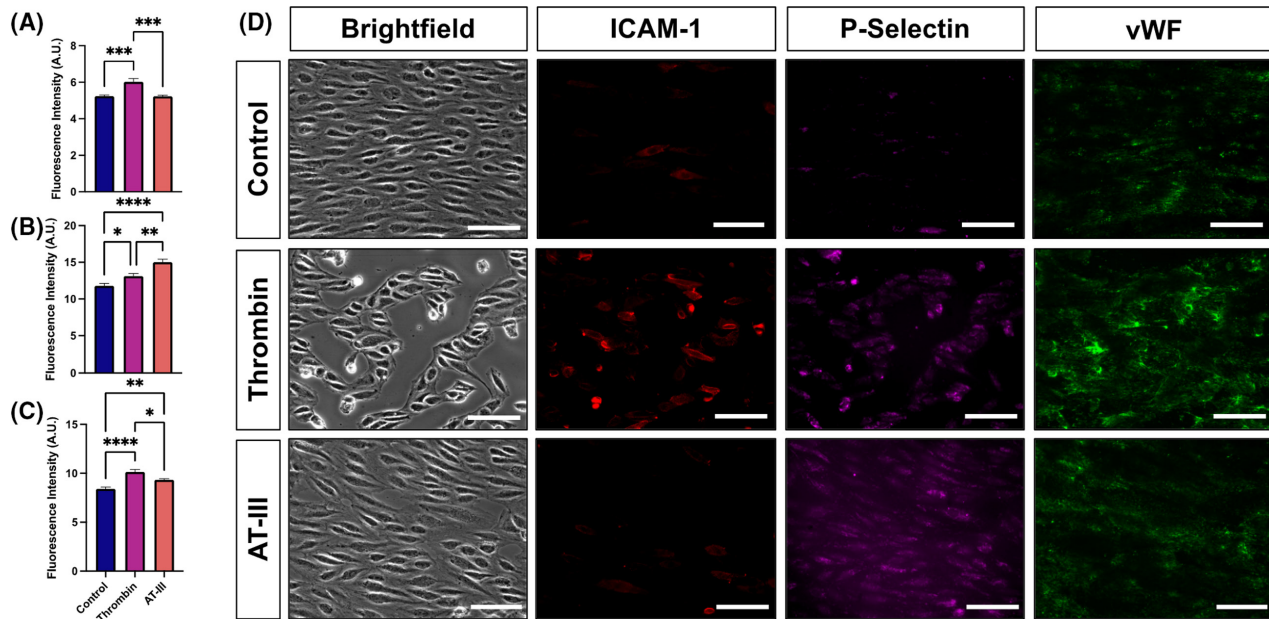


FIGURE 5 Antithrombin-III (AT-III) decreases intercellular cell adhesion molecule-1 (ICAM-1) and von Willebrand Factor (vWF), but increases P-selectin surface expression. Thrombin increases surface expression of (A) ICAM-1 that is rescued by pretreatment with AT-III, while (B) P-selectin is increased in both thrombin and AT-III conditions. (C) Von Willebrand factor is increased in thrombin conditions compared to control and AT-III conditions; AT-III also has significant increased surface expression of vWF when compared to control channels. Representative images of each stain and condition can be seen in (D). Scale bars represent 100 μm. Asterisks are used for significance levels: *, $p \leq 0.05$; **, $p \leq 0.005$; ***, $p \leq 0.0005$; ****, $p \leq 0.0001$. Data were analysed using a one-way analysis of variance (ANOVA) followed by Tukey's multiple comparisons test. [Colour figure can be viewed at [wileyonlinelibrary.com](https://onlinelibrary.wiley.com/doi/10.1111/bjh.18328)]

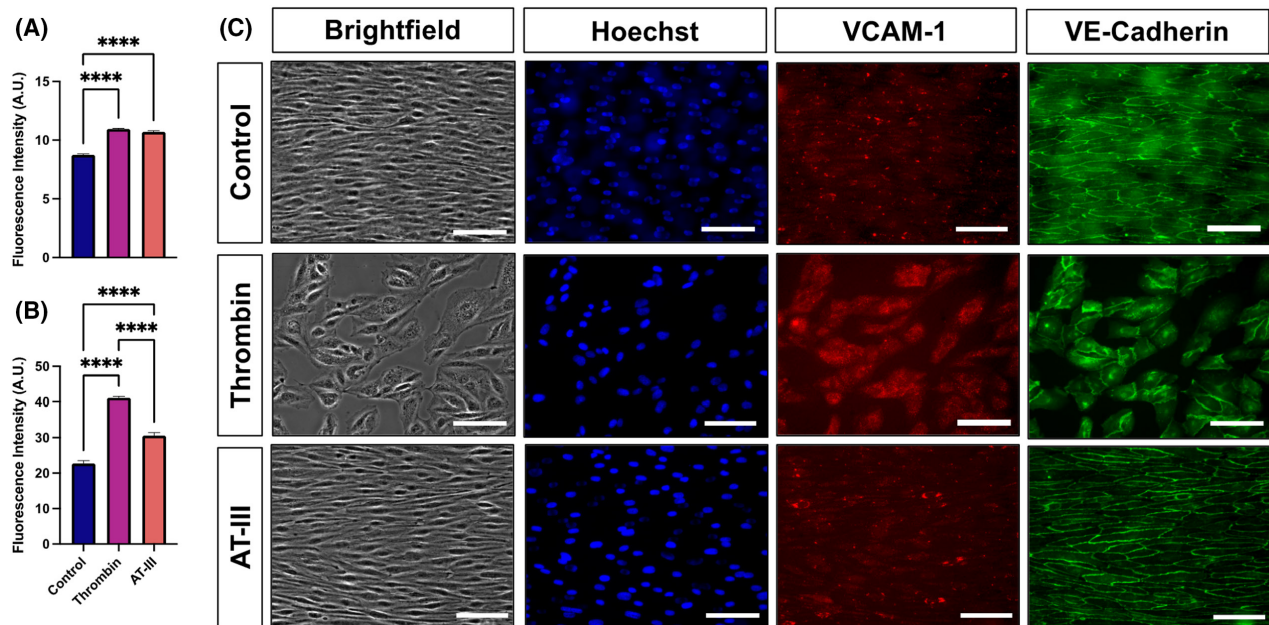


FIGURE 6 Antithrombin-III (AT-III) decreases VE-cadherin surface expression, but does not change vascular cell adhesion molecule-1 (VCAM-1) expression. (A) VCAM-1 surface expression is increased in thrombin and AT-III channels compared to controls. (B) Thrombin increases surface expression of VE-cadherin that is reduced by pretreatment with AT-III. Representative images of each stain and condition can be seen in (C). Scale bars represent 100 μm. Asterisks are used for significance levels: *, $p \leq 0.05$; **, $p \leq 0.005$; ***, $p \leq 0.0005$; ****, $p \leq 0.0001$. Data were analysed using a one-way analysis of variance (ANOVA) followed by Tukey's multiple comparisons test. [Colour figure can be viewed at [wileyonlinelibrary.com](https://onlinelibrary.wiley.com/doi/10.1111/bjh.18328)]

nuclear factor kappa B pathway. It also plays a role as an inhibitor of inflammatory cytokine production and expression of VCAM-1 and furthermore desensitizes the chemokine receptors of leukocytes through binding to syndecan-4.^{33,35}

In our experiments, treating ECs with 7 u/ml ATIII prior to thrombin incubation almost completely prevented the contracted phenotype. ATIII has been shown to bind primarily to heparan sulphate proteoglycans located on the EC

surface.²⁵ In order to verify the mechanism by which ATIII was exerting its effects, we incubated HUVECs with heparinase I prior to ATIII treatment to degrade the heparan sulphate molecules on the EC surface. Results from incubation with heparinase I support the mechanism reported in the literature and illustrated in [Figure 7](#).^{25,37,38}

To determine whether there were significant adhesion events of HbAA RBCs to HUVECs increased after thrombin exposure, we perfused RBC suspensions from healthy donors over control and treated ECs. Adhesion for all conditions was exceedingly low, with thrombin pretreatment showing the highest amount of adhered RBCs. These findings are not surprising since healthy HbAA RBCs are generally considered to be non-adhesive, despite expressing surface adhesion molecules.²⁴ In contrast, HbSS RBCs are widely known to be adhesive to endothelial surfaces. As expected, non-treated (control) HUVECs exhibited very few adhesive HbSS RBCs. Adhesion events greatly increased when HUVECs were activated with thrombin. These adhesion events can trigger vaso-occlusive crisis events that occur throughout the microvasculature of SCD patients.

Since ATIII was able to mitigate the morphological response of ECs to thrombin, we sought to investigate whether it would also prevent HbSS RBCs from adhering to the thrombin-activated HUVEC surface. Indeed, RBC adhesion to control and ATIII microchannels was similar, revealing

the efficacy of ATIII in preventing HbSS RBC adhesion. Our findings support the findings by Gutsaeva *et al.* of reduced adhesion of RBC and white blood cells (WBC) to vascular endothelium in the bone marrow microcirculation of SCD mice by intravital microscopy when the animals were pretreated with ATIII compared to vehicle.³⁹

Thrombin has been shown to induce expression of several types of adhesion molecules on the EC surface, all of which can contribute to HbSS RBC adhesion.^{13,40,41,42} To profile which adhesion molecules were responsible for the increased adhesion observed in our experiments, we used immunofluorescence to stain for several well-known HbSS adhesion molecules ([Figures 5, 6](#)). P-selectin increased with thrombin exposure and even further increased with ATIII pretreatment, yet HbSS RBC adhesion did not show the same pattern of adhesion ([Figure 5B](#)), suggesting P-selectin is not the dominating adhesion molecule mediating RBC adhesion. Several of the adhesion molecules probed showed an increase in expression with thrombin treatment but decreased expression with ATIII pretreatment; these included ICAM-1, vWF, and VCAM-1 ([Figures 5A,C and 6A](#)). We hypothesize that these molecules are the key players in HbSS RBC adhesion since this expression pattern matches that of HbSS adhesion.

Using the endothelium-on-a-chip *in vitro* microfluidic assay, we mimicked the compromised vasculature through

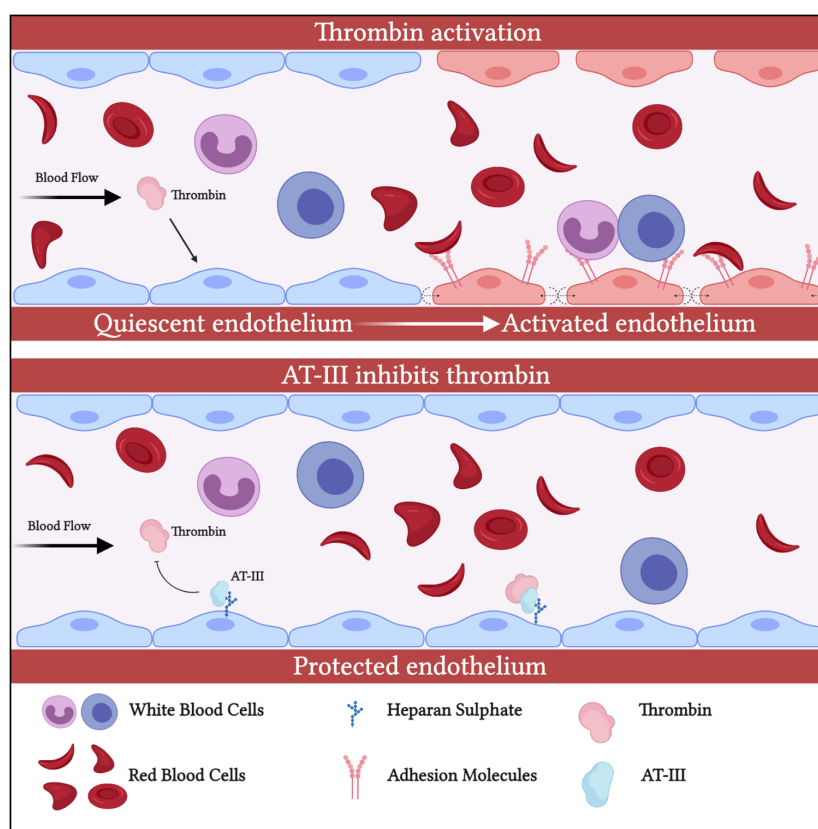


FIGURE 7 Illustration of the mechanisms involved in the endothelium-on-a-chip experiments. The top illustration shows thrombin causing endothelial cell (EC) contraction and blood cell adhesion. The lower panel displays the mechanism of antithrombin III (AT-III) binding to heparan sulphate molecules and protecting the ECs against the effects of thrombin. [Colour figure can be viewed at wileyonlinelibrary.com]

thrombin treatment and demonstrated an increased adhesion of HbSS RBCs as a model of VOs. We report for the first time that ATIII pretreatment of human ECs reduced HbSS RBC adhesion to thrombin-activated endothelium in microscale flow. ATIII mitigated EC contraction and reduced surface expression of von Willebrand factor, which is mediated by thrombin. Our experiments show that prophylactic ATIII may prevent SCD VOs through mitigation of increased thrombin activity. By attenuating EC damage and HbSS RBC adhesion to endothelium, ATIII has alleviated the consequences of thrombin exposure in our *in vitro* model. For SCD patients with elevated thrombin–antithrombin complexes and other evidence of a systemic hypercoagulable state, we speculate that ATIII could be a viable acute or chronic treatment approach. Our findings support the notion that ATIII should be further investigated as a therapeutic for SCD VOs.

AUTHOR CONTRIBUTIONS

Study design: William J. Wulftange, Erdem Kucukal and Umut A. Gurkan; performing experiments: William J. Wulftange, Yuncheng Man, Ran An, Karamoja Monchamp, Charlotte D. Sevrain and Himanshu R. Dashora; data analysis: William J. Wulftange, Erdem Kucukal, Ran An, Himanshu R. Dashora and Umut A. Gurkan; data interpretation: William J. Wulftange, Erdem Kucukal, Yuncheng Man, Ran An, Anton Ilich, Jane A. Little, Nigel S. Key and Umut A. Gurkan; manuscript writing: William J. Wulftange, Erdem Kucukal, Karamoja Monchamp and Amma T. Owusu-Ansah; manuscript editing: Anton Ilich, Jane A. Little, Nigel S. Key and Umut A. Gurkan; clinical samples: Jane A. Little and Allison Bode

ACKNOWLEDGEMENTS

This work was supported by National Heart, Lung, and Blood Institute Awards: R01HL133574, OT2HL152643, U01HL117659, and T32HL134622. This work was also supported by the Clinical and Translational Science Collaborative of Cleveland, UL1TR002548 from the National Center for Advancing Translational Sciences, a component of the National Institutes of Health, and NIH Roadmap for Medical Research, Case-Coulter Translational Research Partnership Program. This work was also supported in part by NIH grant T32 GM007250 and TL1 TR000441. This work was also funded by an Investigator Initiated Grant from Grifols, S.A. The authors acknowledge with gratitude the contributions of patients and clinicians at Seidman Cancer Center (University Hospitals, Cleveland). Umut A. Gurkan acknowledges National Science Foundation CAREER Award 1552782, which supported this study in part. Umut A. Gurkan would like to thank the Case Western Reserve University, University Center for Innovation in Teaching and Education (UCITE) for the Glennan Fellowship, which supports the scientific art program and the art student internship in CASE-BML. Open access funding enabled and organized by ProjektDEAL.

DISCLOSURES

Ran An: *Hemex Health, Inc.*: patents & royalties. Jane A. Little: *NHLBI*: research funding; *GBT*: membership on an entity's Board of Directors or advisory committees; *GBT*: research funding; *Bluebird Bio*: Research Funding; *BioChip Labs*: patents & royalties: SCD Biochip (patent, no royalties); *Hemex Health, Inc.*: patents & royalties: microfluidic electrophoresis (patent, no royalties). Nigel S. Key: *Novo Nordisk*: other: chair of grants committee; *Takeda*: research funding; *Grifols*: research funding; *Uniquire*: consultancy. Umut A. Gurkan: *Hemex Health, Inc.*: consultancy, current employment, patents & royalties, research funding; *BioChip Labs*: patents & royalties; *Dx Now Inc.*: patents & royalties; *Xatek Inc.*: patents & royalties. Erdem Kucukal: *BioChip Labs*: previous employment, patents & royalties.

DATA AVAILABILITY STATEMENT

Data are available upon reasonable request to the corresponding author.

ORCID

William J. Wulftange  <https://orcid.org/0000-0003-0708-3876>

Yuncheng Man  <https://orcid.org/0000-0002-3034-5523>

Ran An  <https://orcid.org/0000-0002-4849-0120>

Anton Ilich  <https://orcid.org/0000-0002-7669-0760>

Nigel S. Key  <https://orcid.org/0000-0002-8930-4304>

Umut A. Gurkan  <https://orcid.org/0000-0002-0331-9960>

REFERENCES

- Salvaggio JE, Arnold CA, Banov CH. Long-term anti-coagulation in sickle-cell disease. A clinical study. *N Engl J Med.* 1963;269:182–6.
- Amin C, Adam S, Mooberry MJ, Kutlar A, Kutlar F, Esserman D, et al. Coagulation activation in sickle cell trait: an exploratory study. *Br J Haematol.* 2015;171(4):638–46.
- Ataga KI, Orringer EP. Hypercoagulability in sickle cell disease: a curious paradox. *Am J Med.* 2003;115(9):721–8.
- Minniti CP, Delaney KM, Gorbach AM, Xu D, Lee CC, Malik N, et al. Vasculopathy, inflammation, and blood flow in leg ulcers of patients with sickle cell anemia. *Am J Hematol.* 2014;89(1):1–6.
- Kato GJ, Steinberg MH, Gladwin MT. Intravascular hemolysis and the pathophysiology of sickle cell disease. *J Clin Invest.* 2017;127(3):750–60.
- Noubououssie D, Key NS, Ataga KI. Coagulation abnormalities of sickle cell disease: relationship with clinical outcomes and the effect of disease modifying therapies. *Blood Rev.* 2016;30(4):245–56.
- Salinas Cisneros G, Thein SL. Recent advances in the treatment of sickle cell disease. *Front Physiol.* 2020;11:435.
- Kapoor S, Little JA, Pecker LH. Advances in the treatment of sickle cell disease. *Mayo Clin Proc.* 2018;93(12):1810–24.
- Byrnes JR, Wolberg AS. Red blood cells in thrombosis. *Blood.* 2017;130(16):1795–9.
- Shet AS, Lizarralde-Iragorri MA, Naik RP. The molecular basis for the prothrombotic state in sickle cell disease. *Haematologica.* 2020;105(10):2368–79.
- Krishnaswamy S. The transition of prothrombin to thrombin. *J Thromb Haemost.* 2013;11(Suppl 1):265–76.
- Link KG, Stobb MT, Sorrells MG, Bortot M, Ruegg K, Manco-Johnson MJ, et al. A mathematical model of coagulation under flow identifies factor V as a modifier of thrombin generation in hemophilia a. *J Thromb Haemost.* 2020;18(2):306–17.

13. Sparkenbaugh EM, Chen C, Brzoska T, Nguyen J, Wang S, Vercellotti GM, et al. Thrombin activation of PAR-1 contributes to microvascular stasis in mouse models of sickle cell disease. *Blood*. 2020;135(20):1783–7.
14. Manodori AB, Matsui NM, Chen JY, Embury SH. Enhanced adherence of sickle erythrocytes to thrombin-treated endothelial cells involves interendothelial cell gap formation. *Blood*. 1998;92(9):3445–54.
15. Manodori AB, Barabino GA, Lubin BH, Kuypers FA. Adherence of phosphatidylserine-exposing erythrocytes to endothelial matrix thrombospondin. *Blood*. 2000;95(4):1293–300.
16. Whelihan MF, Lim MY, Mooberry MJ, Piegore MG, Ilich A, Wogu A, et al. Thrombin generation and cell-dependent hypercoagulability in sickle cell disease. *J Thromb Haemost*. 2016;14(10):1941–52.
17. Qari MH, Aljaouni SK, Alardawi MS, Fatani H, Alsayes FM, Zografos P, et al. Reduction of painful vaso-occlusive crisis of sickle cell anaemia by tinzaparin in a double-blind randomized trial. *Thromb Haemost*. 2007;98(2):392–6.
18. Schreuder HA, de Boer B, Dijkema R, Mulders J, Theunissen HJ, Grootenhuis PD, et al. The intact and cleaved human antithrombin III complex as a model for serpin-proteinase interactions. *Nat Struct Biol*. 1994;1(1):48–54.
19. Kucukal E, Ilich A, Key NS, Little JA, Gurkan UA. Red blood cell adhesion to heme-activated endothelial cells reflects clinical phenotype in sickle cell disease. *Am J Hematol*. 2018;93:1050–60.
20. Kucukal E, Man Y, Hill A, Liu S, Bode A, An R, et al. Whole blood viscosity and red blood cell adhesion: potential biomarkers for targeted and curative therapies in sickle cell disease. *Am J Hematol*. 2020;95:1246–56.
21. Man Y, Goreke U, Kucukal E, Hill A, An R, Liu S, et al. Leukocyte adhesion to P-selectin and the inhibitory role of Crizanlizumab in sickle cell disease: a standardized microfluidic assessment. *Blood Cells Mol Dis*. 2020;83:102424.
22. Kucukal E, Man Y, Quinn E, Tewari N, An R, Ilich A, et al. Red blood cell adhesion to ICAM-1 is mediated by fibrinogen and is associated with right-to-left shunts in sickle cell disease. *Blood Adv*. 2020;4(15):3688–98.
23. Jaccard N, Griffin LD, Keser A, Macown RJ, Super A, Veraitch FS, et al. Automated method for the rapid and precise estimation of adherent cell culture characteristics from phase contrast microscopy images. *Biotechnol Bioeng*. 2014;111(3):504–17.
24. Telen MJ. Red blood cell surface adhesion molecules: their possible roles in normal human physiology and disease. *Semin Hematol*. 2000;37(2):130–42.
25. Opal SM, Kessler CM, Roemisch J, Knaub S. Antithrombin, heparin, and heparan sulfate. *Crit Care Med*. 2002;30(5 Suppl):S325–31.
26. Alapan Y, Kim C, Adhikari A, Gray KE, Gurkan-Cavusoglu E, Little JA, et al. Sickle cell disease biochip: a functional red blood cell adhesion assay for monitoring sickle cell disease. *Transl Res*. 2016;173:74, e8–91.
27. El Nemer W, Wautier MP, Rahuel C, Gane P, Hermand P, Galacteros F, et al. Endothelial Lu/BCAM glycoproteins are novel ligands for red blood cell alpha4beta1 integrin: role in adhesion of sickle red blood cells to endothelial cells. *Blood*. 2007;109(8):3544–51.
28. Setty BN, Stuart MJ. Vascular cell adhesion molecule-1 is involved in mediating hypoxia-induced sickle red blood cell adherence to endothelium: potential role in sickle cell disease. *Blood*. 1996;88(6):2311–20.
29. Hebbel RP. Adhesive interactions of sickle erythrocytes with endothelium. *J Clin Invest*. 1997;100(11 Suppl):S83–6.
30. Pathare A, Kindi SA, Daar S, Dennison D. Cytokines in sickle cell disease. *Hematology*. 2003;8(5):329–37.
31. van Nieuw Amerongen GP, Musters RJ, Eringa EC, Sipkema P, van Hinsbergh VW. Thrombin-induced endothelial barrier disruption in intact microvessels: role of RhoA/rho kinase-myosin phosphatase axis. *Am J Physiol Cell Physiol*. 2008;294(5):C1234–41.
32. Garcia JG, Verin AD, Schaphorst KL. Regulation of thrombin-mediated endothelial cell contraction and permeability. *Semin Thromb Hemost*. 1996;22(4):309–15.
33. Shi S, Verin AD, Schaphorst KL, Gilbert-McClain LI, Patterson CE, Irwin RP, et al. Role of tyrosine phosphorylation in thrombin-induced endothelial cell contraction and barrier function. *Endothelium*. 1998;6(2):153–71.
34. Ghosh S, Tan F, Ofori-Acquah SF. Spatiotemporal dysfunction of the vascular permeability barrier in transgenic mice with sickle cell disease. *Anemia*. 2012;2012:582018.
35. Rezaie AR, Giri H. Anticoagulant and signaling functions of anti-thrombin. *J Thromb Haemost*. 2020;18:3142–53.
36. Noomuna P, Risinger M, Zhou S, Seu K, Man Y, An R, et al. Inhibition of Band 3 tyrosine phosphorylation: a new mechanism for treatment of sickle cell disease. *Br J Haematol*. 2020;190(4):599–609.
37. Mosier PD, Krishnasamy C, Kellogg GE, Desai UR. On the specificity of heparin/heparan sulfate binding to proteins. Anion-binding sites on antithrombin and thrombin are fundamentally different. *PLoS One*. 2012;7(11):e48632.
38. Sasisekharan R, Venkataraman G. Heparin and heparan sulfate: biosynthesis, structure and function. *Curr Opin Chem Biol*. 2000;4(6):626–31.
39. Gutsaeva DR, Yang N, Parkerson JB, Xiao H, Yerigenahally S, Dickerson C, et al. Anti-thrombin III inhibits adhesion of sickle red blood cells and leukocytes to the endothelium in a sickle cell mouse model: potential therapeutic application for Vaso-occlusive episodes. *Blood*. 2016;128(22):2473.
40. Minami T, Aird WC. Thrombin stimulation of the vascular cell adhesion molecule-1 promoter in endothelial cells is mediated by tandem nuclear factor-kappa B and GATA motifs. *J Biol Chem*. 2001;276(50):47632–41.
41. Xue J, Thippogowda PB, Hu G, Bachmaier K, Christman JW, Malik AB, et al. NF-kappaB regulates thrombin-induced ICAM-1 gene expression in cooperation with NFAT by binding to the intronic NF-kappaB site in the ICAM-1 gene. *Physiol Genomics*. 2009;38(1):42–53.
42. Telen MJ. Role of adhesion molecules and vascular endothelium in the pathogenesis of sickle cell disease. *Hematology Am Soc Hematol Educ Program*. 2007;84-90:84–90.

SUPPORTING INFORMATION

Additional supporting information can be found online in the Supporting Information section at the end of this article.

How to cite this article: Wulftange WJ, Kucukal E, Man Y, An R, Monchamp K, Sevrain CD, et al. Antithrombin-III mitigates thrombin-mediated endothelial cell contraction and sickle red blood cell adhesion in microscale flow. *Br J Haematol*. 2022;198:893–902. <https://doi.org/10.1111/bjh.18328>